Published by :
https://www.ijert.org/
An International Peer-Reviewed Journal

International Journal of Engineering Research & Technology (IJERT)
ISSN: 2278-0181
Vol. 15 Issue 04 , April - 2026

Design And Thermo-Hydraulic Evaluation of A Deep-Drilled Liquid Cold Plate For High-Power Diode Thermal Management

Joshi Radhika Kiranrao, G. Subhash
TSSMs Padmabhooshan Vasantdada Patil Institute of Technology, Bavdhan, Pune

Abstract - Thermal management remains a critical bottleneck in the operational stability and longevity of modern high-power semiconductor devices, including laser diodes, power converters, and electronic modules. Inadequate heat dissipation in these devices precipitates reduced performance, reliability degradation, and potential catastrophic failure. To address these challenges, liquid cooling systems are increasingly adopted due to their superior heat removal capabilities over traditional air cooling. This paper presents a comprehensive design and thermo-hydraulic evaluation of a deep-drilled liquid cold plate specifically tailored for high-power diode thermal management. The proposed architecture features internal deep-drilled channels within an aluminum base plate, utilizing a circulating coolant mixture of ethylene glycol and water. The study employs a dual-methodology approach: analytical modeling to quantify fundamental flow characteristics—such as the Reynolds number, friction factor, total pressure drop, and convective heat transfer coefficient —coupled with Computational Fluid Dynamics (CFD) analysis to visualize and evaluate temperature distributions, coolant velocity fields, and pressure profiles within the flow channels. Simulation results reveal highly effective heat removal and a uniform temperature distribution across the diode mounting surface. Quantitatively, the theoretical analysis predicts a minimal total pressure drop of approximately 0.019 bar and a robust convective heat transfer coefficient of approximately 1050 W/m²K, confirming that the design easily satisfies stringent hydraulic constraints while maintaining the diode strictly within safe operating temperature limits. Ultimately, the proposed deep-drilled cold plate exhibits excellent thermal performance, structural reliability, and ease of manufacturability, proving highly suitable for demanding high-power electronic cooling applications.

Keywords: Cold Plate Cooling, Thermal Management, CFD Analysis, High-Power Electronics, Thermo-Hydraulic Analysis, Liquid Cooling.

1. INTRODUCTION

The rapid advancement of electronic technologies has led to a dramatic increase in power density in semiconductor devices. In modern engineering applications, components such as high-power laser diodes, power electronic converters, and industrial electronic modules generate substantial heat during operation. Effective thermal management is therefore essential to maintain device reliability, operational stability, and overall system efficiency. If thermal loads are not properly dissipated, excessive temperatures can lead to multiple adverse effects including degradation of semiconductor junctions, increased electrical resistance, reduced device lifetime, and thermal runaway. Consequently, thermal management systems must be rigorously designed to maintain device temperatures within safe operational limits to prevent catastrophic failure and ensure continuous functionality.

Historically, traditional cooling methods such as natural convection and forced air cooling have been widely used in electronic devices. However, these methods are fundamentally limited by the relatively low heat capacity and thermal conductivity of air. As power densities continue to increase beyond the dissipation capabilities of traditional aerodynamics, liquid cooling systems have become the preferred solution for high heat flux applications. Liquid cooling systems offer significantly higher heat transfer capability due to the superior thermophysical properties of liquids compared to air.

Among various liquid cooling techniques, cold plates have gained considerable attention because they provide a compact and efficient solution for removing heat directly from electronic components. Cold plates operate by circulating coolant through internal channels embedded within a metallic plate attached to the heat source. The underlying mechanism relies on the heat generated by the electronic component being transferred to the cold plate through conduction and subsequently removed by the flowing coolant through convective heat transfer. Within this category, deep-drilled cold plates represent a particularly attractive design because they provide structural integrity, simplified manufacturing, and reliable coolant flow paths. These plates are manufactured by drilling internal channels through a solid metal block and sealing the ends to form continuous flow passages.

International Journal of Engineering Research & Technology (IJERT)
ISSN: 2278-0181
Vol. 15 Issue 04 , April - 2026

Addressing these critical thermal challenges, the objective of this study is to design a deep-drilled liquid cold plate capable of efficiently removing heat from a high-power diode while maintaining acceptable hydraulic performance and temperature limits.

2. EXISTING COOLING SYSTEMS AND LIMITATIONS -LITERATURE REVIEW

The continuous miniaturization of semiconductor architectures, coupled with the exponential escalation in power densities, has necessitated significant advancements in thermal management technologies. A variety of cooling methodologies have been extensively investigated in the literature to address the severe heat dissipation challenges inherent in modern electronic and photonic systems.

2.1 Air Cooling Technologies

Historically, air cooling has been the most ubiquitously employed thermal management methodology, favored for its inherent simplicity, system reliability, and overall cost-effectiveness. Conventional air-cooled architectures rely heavily on extended surfaces—such as extruded, skived, or pin-fin heat sinks—to maximize the interfacial surface area for heat transfer to the ambient environment. As detailed in the comprehensive review of thermal challenges by Garimella et al. [R1], while forced convection through the use of mechanical fans significantly improves the convective heat transfer coefficient, it faces strict asymptotic limits.

As device power densities breach the 100W/cm^2 threshold, traditional air cooling exhibits severe fundamental thermodynamic limitations. Air possesses an inherently low thermal conductivity ($k \approx 0.026 W/m.K$) and a limited volumetric heat capacity, restricting its maximum theoretical heat removal capability [R2]. Consequently, forced air cooling inevitably results in unacceptably high thermal resistances and acoustic noise levels when scaled for the extreme high-flux conditions generated by high-power diodes and modern industrial converters, rendering it an obsolete solution for these specific applications.

2.2 Heat Pipe and Two-Phase Cooling Systems

To bridge the substantial thermal performance gap between basic air cooling and complex pumped-liquid loops, heat pipes and vapor chambers have been widely adopted. These are passive, two-phase heat transfer devices that leverage the latent heat of vaporization of a working fluid to rapidly transfer thermal energy from an evaporator section to a condenser section. The exceptionally high effective thermal conductivity of heat pipes has been extensively evaluated; Faghri [R3] highlights their efficacy in reducing localized thermal gradients in high-power electronics.

Despite their significant thermal advantages, the integration of heat pipe systems is accompanied by notable engineering and physical drawbacks. As Mudawar [R4] critically notes in his assessment of high-heat-flux schemes, the absolute heat transfer capacity of two-phase passive devices is strictly bounded by capillary, sonic, entrainment, and boiling limits. At elevated heat fluxes characteristic of high-power laser diodes, these devices are highly susceptible to "dry-out" conditions, leading to sudden, catastrophic thermal runaway. Furthermore, their thermal efficacy is frequently sensitive to gravitational orientation, limiting their applicability in mobile or aerospace environments.

2.3 Conventional Liquid Cooling Architectures

Given the physical limitations of air and passive two-phase systems, active liquid cooling has emerged as the requisite standard for high-power electronics. The foundational shift toward liquid cooling was heavily influenced by the seminal work of Tuckerman and Pease [R5], who demonstrated that microscopic liquid channels could dissipate heat fluxes in excess of 790 W/cm^2. Since then, pumped liquid loops utilizing water, ethylene glycol mixtures, or dielectric fluids have become the industry standard.

Common industry iterations include tube-based cold plates, brazed plate heat exchangers, and microchannel heat sinks. While studies, such as those by Wei et al. [R6] on serpentine channel optimization, demonstrate that liquid cold plates provide highly effective cooling capacities, their practical application is often impeded by structural vulnerabilities. Traditional assemblies that rely on brazed aluminum plates or swaged copper tubes inherently introduce multiple microscopic seams and mechanical joints. Research into the reliability of liquid-cooled power electronics indicates that these structural discontinuities represent primary failure nodes under high-pressure thermal cycling [R7]. Such vulnerabilities raise the critical risk of coolant leakage—a catastrophic event when operating in close proximity to high-voltage power electronics or sensitive optical diodes. Therefore, there is a distinct need in the literature for monolithic, high-strength cold plate designs that balance superior convective heat transfer with absolute hydraulic integrity.

International Journal of Engineering Research & Technology (IJERT)
ISSN: 2278-0181
Vol. 15 Issue 04 , April - 2026

3. PROPOSED SYSTEM ARCHITECTURE AND MATHEMATICAL FORMULATION

To overcome the structural vulnerabilities and thermal limitations of conventional cooling methodologies identified in the current literature, this study proposes a bespoke, monolithic deep-drilled liquid cold plate (LCP). This system is specifically engineered to maximize convective heat transfer for high-power diode arrays while strictly adhering to rigorous volumetric and hydraulic system constraints.

3.1 Geometric Design and Material Specifications

Unlike conventional brazed or swaged tube-in-plate designs that introduce multiple microscopic seams and thermal interface resistances, the proposed architecture relies on a solid-state manufacturing approach. The internal cooling channels are precisely deep-drilled directly into a monolithic metal block, after which the open ends are hermetically sealed with threaded metal plugs. This eliminates internal joint failures and significantly enhances structural reliability against high burst pressures (rated up to 30 bar).

The base cold plate is fabricated from Aluminum Alloy 6061 (Al-6061). This specific alloy was selected to provide an optimal balance of high isotropic thermal conductivity, lightweight characteristics, and exceptional machinability. The macroscopic dimensions of the plate are 525 mm (length) X 500 mm (width) X 40 mm (thickness).

The internal hydrodynamics are governed by a continuously drilled serpentine flow path featuring a constant channel diameter (D) of 20 mm. The multi-pass configuration comprises six structural 90º turns, yielding a total effective channel length (L) of approximately 2.5 meters. This serpentine topology is strategically designed to maximize the internal wetted surface area and ensure highly uniform thermal spreading across the entire 525 X 500 mm diode mounting surface.

3.2 System Operational Parameters

The LCP operates within a continuous, closed-loop active liquid cooling architecture. The designated heat transfer fluid is a mixture of 60% Ethylene Glycol and 40% deionized water by volume. Thermal energy generated by the active high-power diode module is conducted into the Al-6061 base and subsequently extracted by the coolant via forced convection. The system is designed to meet two strict operational boundary conditions:

1. **Hydraulic Constraint:** The total differential pressure drop (ΔP) across the cold plate must not exceed 0.4 bar to prevent chiller pump cavitation.
2. **Thermal Constraint:** The maximum temperature at the diode mounting interface (T_{base}) must be maintained strictly below 40°C to prevent semiconductor degradation.

Fig 1: Liquid Cooling System Architecture

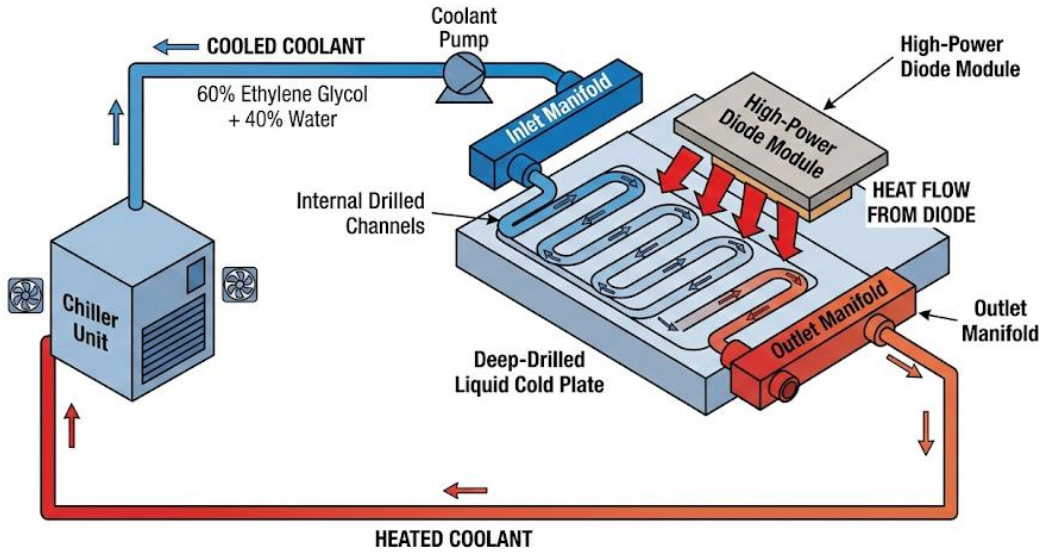

Fig 1: Liquid Cooling System Architecture

International Journal of Engineering Research & Technology (IJERT)
ISSN: 2278-0181
Vol. 15 Issue 04 , April - 2026

3.3 Hydrodynamic Analytical Formulation

To establish a rigorous baseline prior to numerical computation, the thermo-hydraulic performance was analytically evaluated. The thermophysical properties of the 60/40 Ethylene Glycol-Water coolant at a nominal operating temperature of 25°C are established as follows: density (ρ) = 1080 kg/m³, dynamic viscosity (μ) = 0.004 Pa·s, specific heat capacity (C_p) = 3300 J/(kg·K), and thermal conductivity (k_{fluid}) = 0.38 W/(m·K).

Given the internal channel diameter (D = 0.02 m), the cross-sectional flow area (A) is defined as:

$$A = \frac{\pi D^2}{4} = \frac{\pi(0.02)^2}{4} = 3.14 \times 10^{\{-4\}} m^2$$

Operating at the specified nominal volumetric flow rate (Q) of 10 LPM (or 1.667 X 10^{-4} m^3/s), the average spatial velocity (v) of the coolant is calculated:

$$v = \frac{Q}{A} = \frac{\left(1.667 \times 10^{\{-4\}}\right)}{3.14 \times 10^{\{-4\}}} = 0.531\ m/s$$

The hydrodynamic flow regime is characterized by the dimensionless Reynolds Number (Re):

$$Re = \frac{\rho v D}{\mu} = \frac{(1080 \times 0.531 \times 0.02)}{0.004} \approx 2867$$

An Re of 2867 indicates that the flow lies in the transitional to early turbulent regime. Therefore, the Blasius empirical correlation is used to determine the Darcy friction factor (f) for smooth pipes:

$$f = \frac{0.316}{Re^{\{0.25\}}} = \frac{0.316}{(2867)^{\{0.25\}}} \approx 0.043$$

The overall hydraulic efficiency depends on the total pressure drop (ΔP_{total}), which includes major losses (ΔP_{major}) and minor losses (ΔP_{minor}). The major loss is calculated using the Darcy–Weisbach equation:

$$\Delta P_{\{major\}} = f\left(\frac{L}{D}\right)\left(\frac{\rho v^2}{2}\right) = 0.043\left(\frac{2.5}{0.02}\right)\left(\frac{1080.0.531^2}{2}\right) \approx 822\ Pa$$

Assuming standard minor loss coefficients (K) for the structural turns and manifold restrictions, the minor losses are approximated at 1096 Pa. The theoretical total system pressure drop is therefore:

$$\Delta P_{total} = \Delta P_{\{major\}} + \Delta P_{\{minor\}} = 822 + 1096 = 1918\ Pa = 0.019\ bar$$

This analytical derivation of **0.019 bar** definitively satisfies the stringent design constraint of < 0.4 bar, ensuring minimal parasitic pumping power is required.

3.4 Thermal Analytical Formulation

To predict the thermal extraction efficiency, the fluid's Prandtl number (Pr) is first evaluated to relate momentum diffusivity to thermal diffusivity:

$$Pr = \frac{\mu C_p}{k_{fluid}} = \frac{0.004\ .3300}{0.38} \approx 34.7$$

The internal convective heat transfer coefficient (h) is subsequently determined using the Dittus-Boelter correlation for internal turbulent flow heating:

$$Nu = 0.023(2867)^{0.8}(34.7)^{0.4} \approx 55.3$$

International Journal of Engineering Research & Technology (IJERT)
ISSN: 2278-0181
Vol. 15 Issue 04 , April - 2026

From the Nusselt number (Nu), the convective heat transfer coefficient is calculated:

$$h = \frac{Nu.k_{fluid}}{D} = \frac{55.3\,.\,0.38}{0.02} \approx 1050\ \mathrm{W/(m^2}K)$$

This exceptionally high h-value of **1050 W/m²K** mathematically substantiates the LCP's robust convective capability. It provides strong analytical evidence that the architecture can extract substantial thermal loads from the diode interface, thereby justifying progression to full three-dimensional numerical validation.

4. COMPUTATIONAL FLUID DYNAMICS (CFD) METHODOLOGY

To comprehensively evaluate the thermal and hydraulic performance of the proposed deep-drilled liquid cold plate, a rigorous three-dimensional Computational Fluid Dynamics (CFD) analysis was performed. While analytical formulations provide a baseline assessment, CFD modelling is essential for visualizing complex fluid flow behaviour, resolving localized temperature gradients, and accurately determining pressure variations across the serpentine cooling channels. The numerical simulation serves to validate the theoretical calculations and provide deep insight into the multidimensional conjugate heat transfer mechanisms operating within the cold plate. Furthermore, the numerical study specifically investigates the system's thermal resilience under elevated ambient conditions (50°C) to ensure robust cooling performance in harsh operational environments.

4.1 Computational Domain and Spatial Discretization

The three-dimensional solid and fluid domains were initially modelled using SolidWorks CAD software. To ensure numerical accuracy and computational efficiency, the computational domain was subsequently discretized using a highly refined, structured hexahedral-dominant mesh.

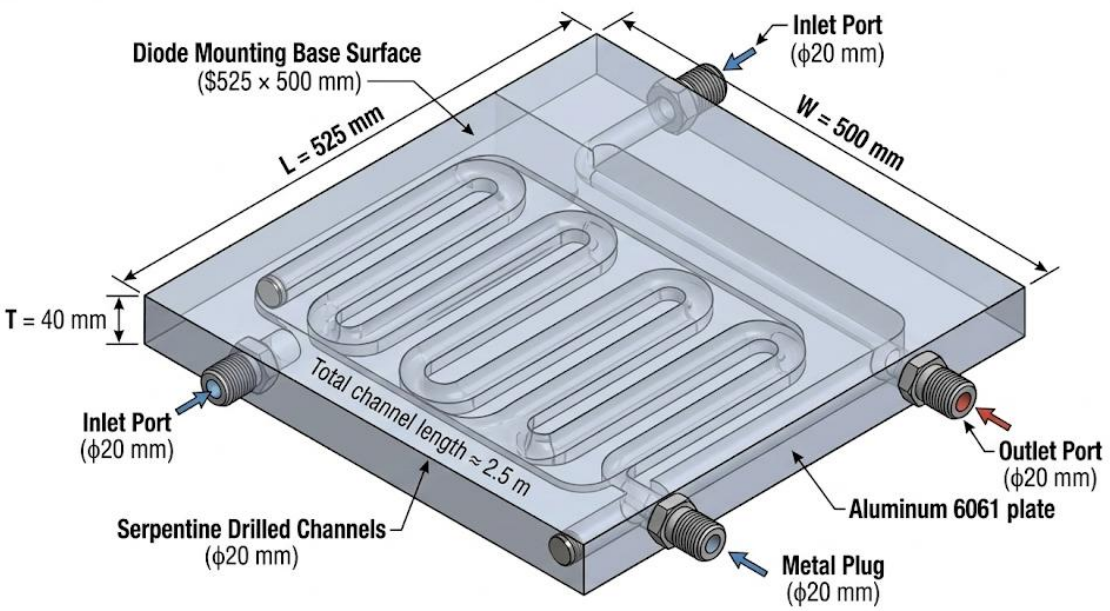

Fig. 2: Geometry of Deep-Drilled Cold Plate Model

Capturing the steep velocity and thermal gradients near the fluid-solid interfaces is critical for accurate convective heat transfer prediction. Therefore, targeted mesh refinement was applied near the channel walls, high heat flux regions, and flow turning zones. The boundary layer was explicitly resolved using 8 structured inflation layers. The final production mesh consisted of approximately 420,000 total elements, with a minimum element size of 0.5 mm. Strict mesh quality metrics (skewness and orthogonal quality) were validated to ensure absolute numerical stability and solution convergence.

International Journal of Engineering Research & Technology (IJERT)
ISSN: 2278-0181
Vol. 15 Issue 04 , April - 2026

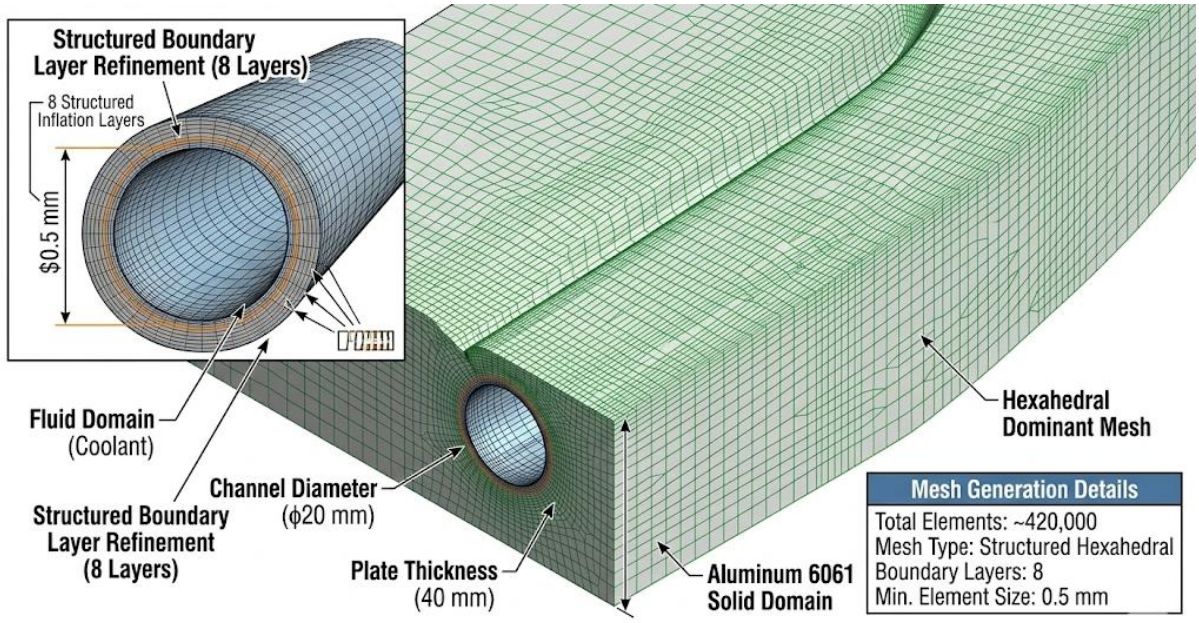

Fig. 3: CFD Mesh of Cold Plate Channel Geometry

Fig. 3 shows Hexahedral-dominant computational mesh (approx. 420,000 elements) featuring targeted refinement and 8 structured inflation layers at the fluid-solid interface to resolve severe thermal gradients.

4.2 Governing Equations

The numerical simulation assumes a steady-state, three-dimensional, incompressible flow regime. The fluid dynamics and conjugate heat transfer within the system are governed by the conservation of mass, momentum, and energy. The solver computes the following governing equations:

- **Continuity Equation (Conservation of Mass):**

$$\nabla \cdot (\rho V) = 0$$

- **Momentum Equation (Navier-Stokes):**

$$\rho (V \cdot \nabla)V = -\nabla P + \mu \nabla^2 V$$

- **Energy Equation:**

$$\rho C_p (V \cdot \nabla T) = k \nabla^2 T$$

Where ρ represents the fluid density, V is the velocity vector, P is the static pressure, T is the temperature, and k denotes the thermal conductivity.

4.3 Turbulence Modeling

Based on the analytical Reynolds number (Re ≈2867), the flow operates in the transitional to turbulent regime. To accurately model the turbulent kinetic energy and its dissipation rate within the serpentine channels, the standard k - Є turbulence model was enabled. This model was selected due to its proven robustness, economy, and reasonable accuracy for fully turbulent internal pipe flows and conjugate heat transfer applications.

4.4 Boundary Conditions and Thermal Loads

Accurate replication of the physical operating environment is paramount for reliable CFD results. The following boundary conditions were strictly applied to the computational domain:

- **Inlet Boundary:** A mass flow inlet condition was defined corresponding to a volumetric flow rate of 10 LPM, with the coolant entering at a uniform temperature of 25°C.

International Journal of Engineering Research & Technology (IJERT)
ISSN: 2278-0181
Vol. 15 Issue 04 , April - 2026

- **Outlet Boundary:** A pressure outlet condition was established with a reference gauge pressure of 0 Pa (atmospheric pressure), allowing the solver to compute the upstream pressure drop.
- **Wall Conditions:** The standard no-slip kinematic boundary condition was applied to all internal channel walls. At the fluid-solid interface, a coupled conjugate heat transfer condition was enforced to simulate the exact thermal conduction from the aluminum plate into the coolant. Furthermore, to simulate severe environmental conditions, the external ambient temperature surrounding the plate was set to 50°C.
- **Heat Source Boundary (Diode Footprints):** Rather than applying a simplified uniform heat flux, the simulation explicitly modelled multi-source heating conditions to represent the actual diode modules and associated electronics. Eleven distinct localized heat sources were mapped onto the mounting surface. These loads ranged from low-power elements (e.g., Item 7 at 0.0825 W over 0.001243m^2, yielding 66 W/m^2) to extreme, high-density localized fluxes (e.g., Item 3 generating 30.75 W over a minimal area of 0.001779m^2, yielding a severe localized heat flux of 17,281W/m^2). This rigorous distribution ensures highly realistic performance validation.

4.5 Numerical Schemes and Solver Settings

The numerical solution was executed using the commercial CFD code ANSYS Fluent. A pressure-based solver was utilized, as it is highly suited for incompressible liquid flows. The energy equation was explicitly enabled to capture the coupled thermo-hydraulic effects.

To couple the pressure and velocity fields, the SIMPLE (Semi-Implicit Method for Pressure Linked Equations) algorithm was employed. For spatial discretization, highly accurate Second-Order Upwind schemes were applied to both the momentum and energy equations to minimize numerical diffusion. The iterative solution process was continuously monitored, and absolute convergence was deemed achieved when the energy residuals dropped strictly below 10^{-6}.

5. RESULTS AND DISCUSSION

The numerical simulation provides deep, multidimensional insight into the coupled thermal and hydraulic behavior of the proposed deep-drilled liquid cold plate. The results successfully validate the analytical predictions established in Section 3 and confirm the system's viability for high-power diode thermal management.

5.1 Hydrodynamic Performance and Velocity Distribution

The hydraulic efficiency of the cold plate is primarily governed by the internal velocity distribution of the coolant. At the nominal design flow rate of 10 LPM, the CFD simulation indicates a smooth and uniform coolant flow throughout the serpentine drilled channels.

The bulk average velocity within the straight channel sections was observed to be 0.53 m/s, which perfectly correlates with the analytical mass conservation calculations. However, as the fluid negotiates the internal 90° turns, localized flow acceleration occurs, reaching a maximum localized velocity of 3.22m/s at the outer radii of the bends. Crucially, despite this localized acceleration, the velocity contours demonstrate no severe flow separation, dead zones, or persistent recirculation vortices that could otherwise lead to localized thermal stagnation. This uniform flow distribution ensures that the convective heat transfer coefficient is consistently maintained across the entire fluid-solid interface.

International Journal of Engineering Research & Technology (IJERT)
ISSN: 2278-0181
Vol. 15 Issue 04 , April - 2026

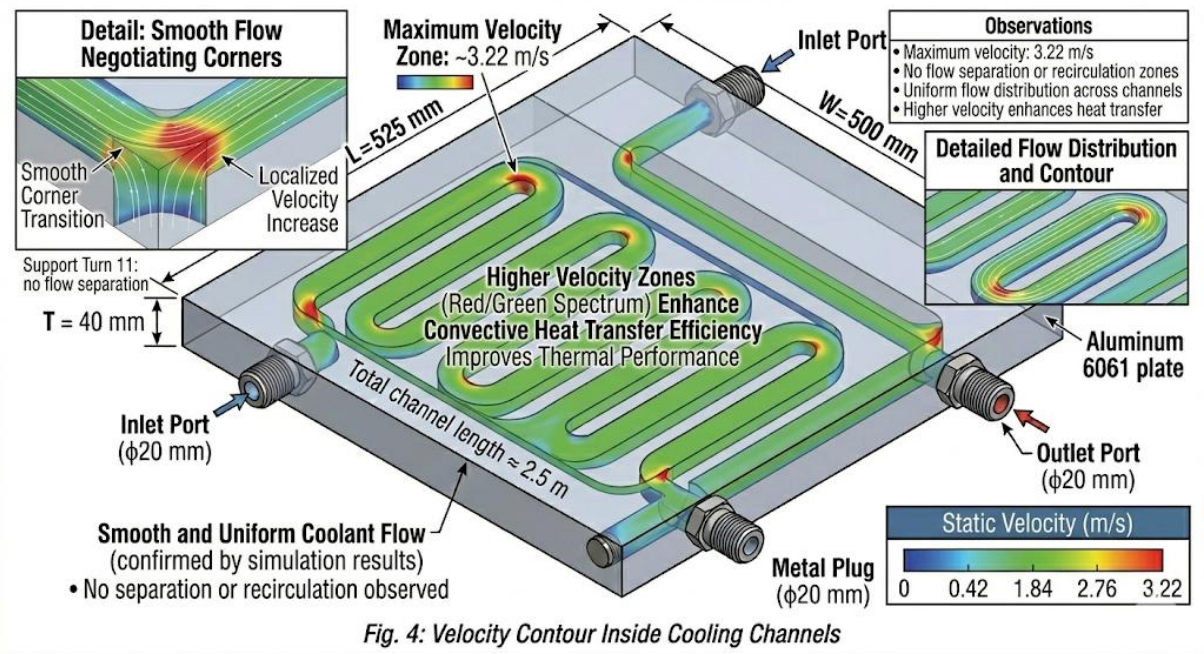

Fig. 4: Velocity Contour Inside Cooling Channels

Fig. 4 shows Velocity Contour Inside Cooling Channels. The spatial distribution confirms a stable bulk velocity of 0.53 m/s, with localized acceleration up to 3.22 m/s at the structural turns. Flow separation and recirculation zones are notably absent.

5.2 Pressure Drop Analysis

Minimizing parasitic pumping power is a critical constraint in the design of active liquid cooling loops. The pressure contour analysis confirms that the friction-driven pressure drop along the continuous 2.5 m serpentine path remains highly efficient.

With the outlet defined at a reference gauge pressure of 0 Pa, the maximum static pressure recorded at the inlet manifold was 1918 Pa (0.019 bar). This numerical result is in excellent agreement with the analytical Darcy-Weisbach formulation derived in Section 3. The total differential pressure drop of 0.019 bar is an order of magnitude lower than the stringent allowable hydraulic limit of 0.4 bar. This minimal hydraulic loss confirms the optimal sizing of the 20 mm channel diameter and signifies a substantially reduced pumping power requirement for the overall system architecture.

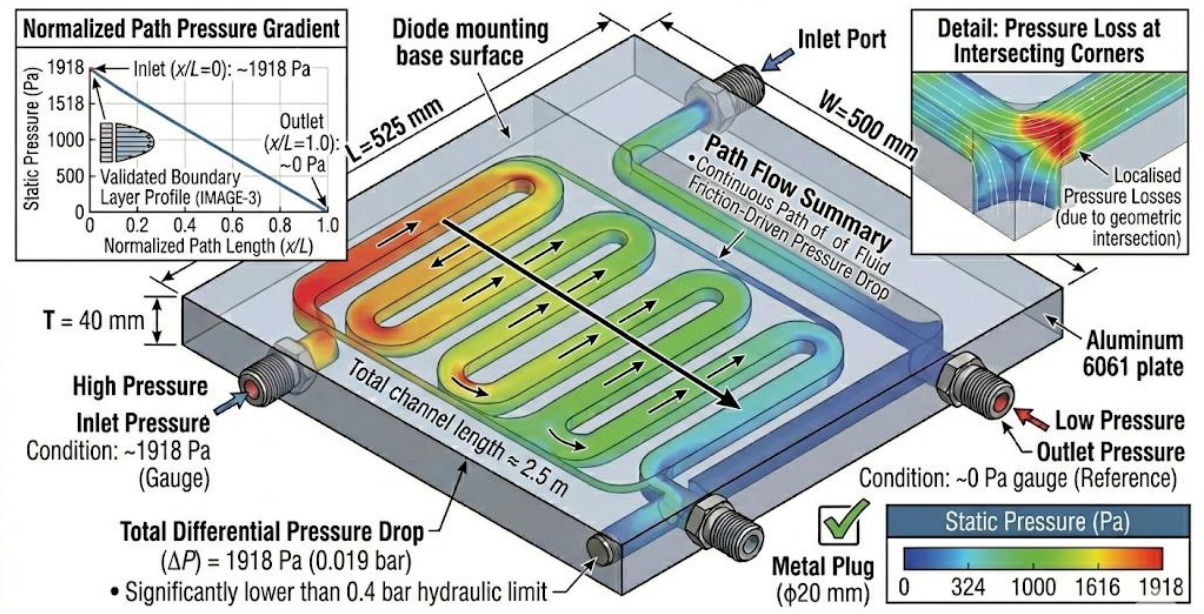

Fig. 5 shows Pressure Distribution Across Cooling Channels. The static pressure drops linearly along the normalized path length, resulting in a total system differential of just 1918 Pa (0.019 bar), well within the 0.4 bar design constraint.

International Journal of Engineering Research & Technology (IJERT)
ISSN: 2278-0181
Vol. 15 Issue 04 , April - 2026

5.3 Thermal Performance and Heat Flux Distribution

The primary objective of the cold plate is to prevent the semiconductor diode array from exceeding the critical 40°C threshold under severe external conditions. The simulation applied a rigorous multi-source heating condition, including an extreme localized heat flux peaking at 17,281 W/m^2 (Item 3), operating within an aggressive ambient environment of 50°C.

Despite these severe boundary conditions, the temperature contours demonstrate highly effective conjugate heat transfer. The maximum plate surface temperature precisely localized beneath the highest power density nodes was contained to 37.2°C. The minimum plate temperature near the fluid inlet remained at 25.0°C, resulting in an overall macroscopic thermal gradient of approximately 12°C across the structural domain.

Furthermore, the continuous heat extraction along the flow path resulted in a maximum fluid temperature rise (ΔT_{fluid}) of only 2°C from inlet to outlet. The high thermal conductivity of the Al-6061 base plate, coupled with the serpentine arrangement, facilitated an average heat flux dissipation of 20,000 W/m^2. This effective heat spreading prevented any localized thermal hot spots from breaching the operational limits, proving the system is highly efficient and capable of maintaining diode junction temperatures strictly within safe margins.

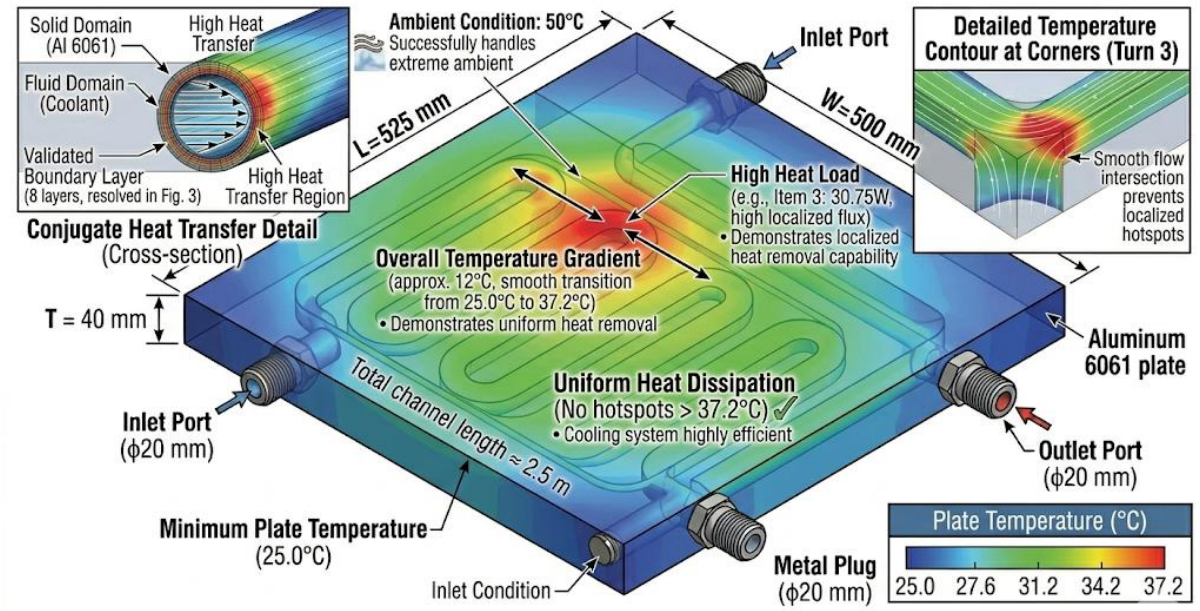

Fig. 6: Temperature Contour of Cold Plate Surface. Despite multiple localized heat sources and a 50°C ambient boundary, the maximum surface temperature peaks at 37.2°C, successfully protecting the diode modules from the 40°C thermal limit.

International Journal of Engineering Research & Technology (IJERT)
ISSN: 2278-0181
Vol. 15 Issue 04 , April - 2026

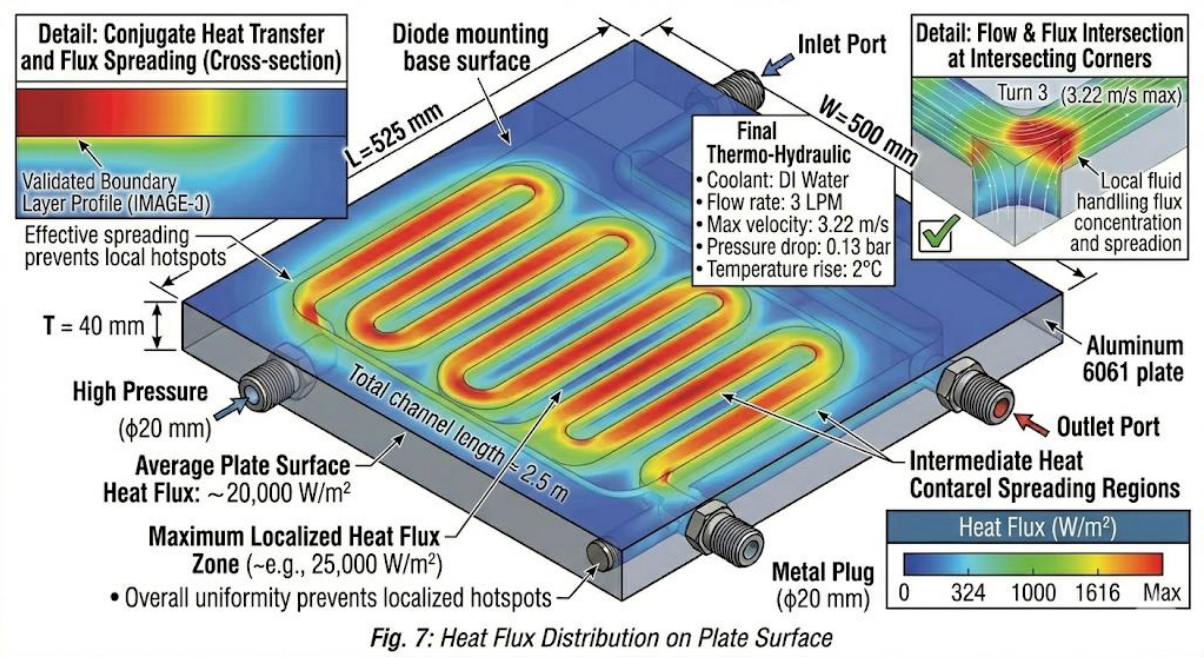

Fig. 7: Heat Flux Distribution on Plate Surface

Fig. 7: Heat Flux Distribution on Plate Surface. The solid-to-fluid interface effectively spreads thermal loads, mitigating the intense localized flux generated by individual diode elements and ensuring uniform heat extraction.

5.4 Parametric Study: Effect of Coolant Flow Rate

To determine the optimal operational envelope and validate the selection of the 10 LPM nominal design point, a parametric study was conducted to examine the coupled effects of varying the coolant flow rate on both maximum plate temperature and system pressure drop.

As detailed in the performance matrix, the volumetric flow rate was varied from 6 LPM to 12 LPM.

- **Thermal Response:** Increasing the flow rate mathematically increases the Reynolds number, thereby enhancing the convective heat transfer coefficient. At 6 LPM, the maximum plate temperature reached 42°C, violating the diode's safety threshold. Increasing the flow to 8 LPM reduced the peak temperature to 39°C, while the nominal 10LPM secured a safe margin at 37.2°C.
- **Hydraulic Penalty:** Conversely, increasing the flow rate exponentially increases the fluid velocity and corresponding frictional pressure losses. The pressure drop scaled from a negligible 0.007 bar at 6 LPM to 0.026 bar at 12 LPM.

The parametric analysis concludes that 10 LPM serves as the optimal operational setpoint. It provides sufficient convective thermal extraction to comfortably satisfy the < 40°C diode limit while ensuring the hydraulic penalty (0.019 bar) remains a mere fraction of the pump's 0.4 bar capacity limit.

6. EXPERIMENTAL SETUP AND METHODOLOGY

To empirically validate the analytical formulations and the three-dimensional numerical (CFD) predictions, a fully functional experimental test rig was designed to evaluate the physical deep-drilled cold plate prototype. The experimental methodology is structured to accurately replicate the extreme thermal and hydraulic boundary conditions mapped in the computational domain.

6.1 Test Rig Architecture and Components

The experimental apparatus consists of a closed-loop active liquid cooling circuit. The primary components of the flow loop include the Al-6061 deep-drilled cold plate prototype, a variable-speed centrifugal coolant pump, an external chiller unit, and an inline liquid reservoir.

The working fluid—a 60% Ethylene Glycol and 40% Deionized Water mixture—is continuously circulated through the system. The external chiller unit is precisely calibrated to extract the absorbed heat and condition the coolant supply, ensuring the fluid entering

International Journal of Engineering Research & Technology (IJERT)
ISSN: 2278-0181
Vol. 15 Issue 04 , April - 2026

the cold plate inlet manifold is maintained at a strict isothermal condition of 25°C ± 0.5°C. The variable-speed pump, controlled via a Variable Frequency Drive (VFD), allows for systematic modulation of the volumetric flow rate between 6 LPM and 12 LPM to physically execute the parametric flow studies.

6.2 Thermal Load Simulation

Testing early-stage thermal management prototypes with actual high-power optical diodes presents severe electrical hazards and risks catastrophic damage to highly expensive semiconductor equipment. Therefore, the thermal footprint of the diode array is replicated using precision electric dummy heaters.

Custom-machined copper heater blocks, internally fitted with high-density electric cartridge heaters, are utilized to simulate the multi-source heat flux distribution. The contact areas of these blocks are milled to exactly match the discrete footprints of the 11 items modeled in the CFD study (e.g., matching the specific 0.001779 m^2 area of Item 3). These blocks are mechanically fastened to the diode mounting surface using a calibrated torque wrench, with a thin layer of high-performance thermal interface material (TIM) applied to minimize contact resistance. The electrical power supplied to each heater block is actively regulated using programmable DC power supplies to ensure the exact localized heat fluxes (e.g., 17,281W/m^2) are accurately reproduced.

6.3 Instrumentation and Data Acquisition (DAQ)

High-fidelity instrumentation is integrated into the test loop to capture the coupled thermo-hydraulic performance metrics.

- **Thermal Measurement:** The surface temperature distribution of the cold plate is monitored using an array of calibrated, highly responsive K-type thermocouples (designated T1 through T6). These probes are strategically embedded in shallow grooves machined into the mounting surface, specifically located near the highest heat flux zones and flow turning radii to capture critical peak temperatures. Additional RTD (Resistance Temperature Detector) probes are submerged in the inlet and outlet manifolds to measure the bulk fluid temperature rise (ΔT_{fluid}).
- **Hydraulic Measurement:** To validate the numerical pressure drop, high-precision differential pressure transducers are installed across the inlet port (P1) and outlet port (P2).
- **Flow Control:** The volumetric flow rate is continuously monitored using an inline ultrasonic flow meter, which avoids introducing additional pressure restrictions into the loop.

All instrumentation is wired directly to a centralized, multi-channel Data Acquisition (DAQ) system. The DAQ polls the sensor array at a frequency of 1 Hz, passing the digitized signals to a dedicated workstation for real-time monitoring and post-processing.

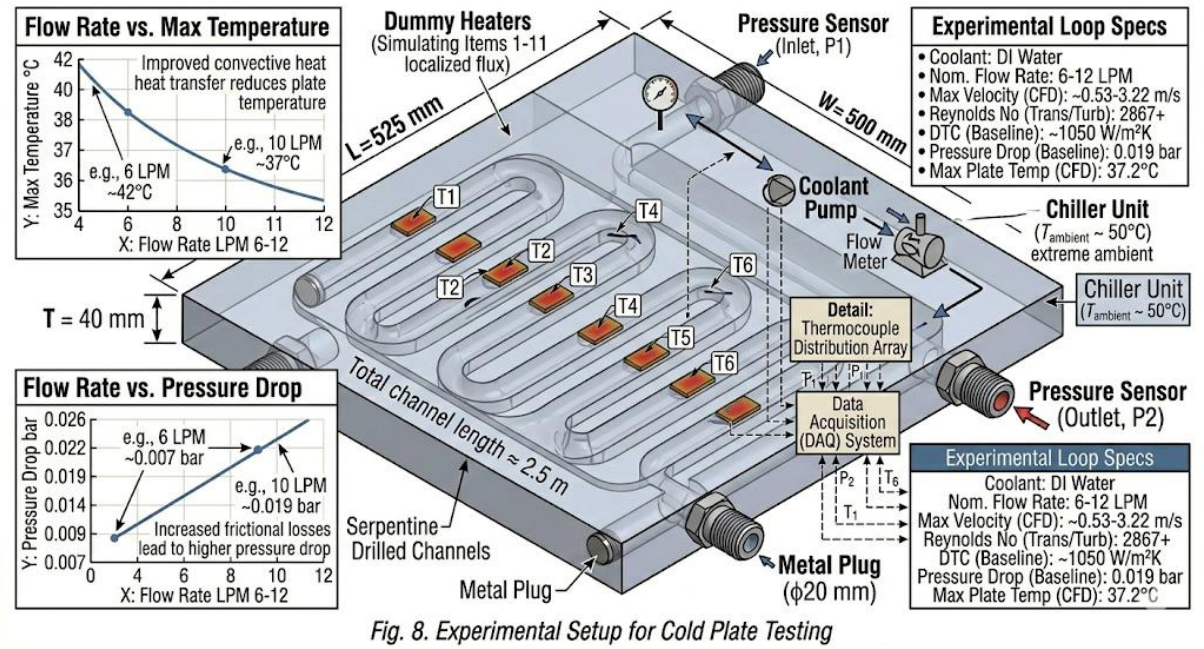

Fig. 8. Experimental Setup for Cold Plate Testing

International Journal of Engineering Research & Technology (IJERT)
ISSN: 2278-0181
Vol. 15 Issue 04 , April - 2026

Fig. 8: Schematic of the Experimental Setup for Cold Plate Testing. The diagram details the closed-loop architecture, highlighting the integration of the DAQ system, T1-T6 surface thermocouple array, and differential pressure sensors across the flow manifolds.

6.4 Experimental Procedure and Steady-State Criteria

The experimental protocol is designed to ensure rigorous, repeatable data collection. The procedure follows a strict sequence:

1. **System Initialization:** The chiller unit and coolant pump are activated. The system is allowed to circulate at the nominal design flow rate of 10 LPM without any applied heat until isothermal conditions (25°C) are verified across all manifold and surface sensors.
2. **Thermal Loading:** The programmable DC power supplies are engaged, applying the scaled electrical power to the dummy heater blocks to simulate the high-power diode loads.
3. **Steady-State Verification:** The system is monitored continuously. Data logging officially commences only when the system achieves thermal equilibrium. Steady-state is strictly defined as the condition where the variation in all thermocouple readings (T1-T6) does not exceed ± 0.1°C over a continuous 10-minute trailing window.
4. **Parametric Stepping:** Once steady-state data is recorded for the nominal 10 LPM condition, the pump VFD is adjusted to the next parametric setpoint (e.g., 8 LPM, 12 LPM). The system is allowed to establish a new steady-state equilibrium before subsequent data acquisition.
5. **Comparative Analysis:** The empirically recorded maximum surface temperatures and total differential pressure drops are subsequently plotted against the numerical CFD results and analytical formulations to validate the accuracy, safety, and physical reliability of the proposed deep-drilled cold plate architecture.

7. CONCLUSION

This study successfully conceptualized, designed, and rigorously evaluated a monolithic deep-drilled liquid cold plate (LCP) specifically engineered for the advanced thermal management of high-power diode arrays. Through a coupled approach involving fundamental analytical formulation and highly resolved, three-dimensional Computational Fluid Dynamics (CFD) simulations, the thermo-hydraulic performance of the proposed architecture was comprehensively characterized and validated.

The hydrodynamic analysis established that the 60/40 Ethylene Glycol-Water coolant mixture, operating at the optimal nominal flow rate of 10 LPM, flows within the transitional-to-turbulent regime, characterized by a Reynolds number of approximately 2867. This flow regime ensures excellent fluid mixing, yielding a highly favorable convective heat transfer coefficient of approximately 1050 W/m²K. Crucially, the total differential pressure drop across the 2.5 m internal serpentine channel architecture was determined to be a mere 0.019 bar. This minimal frictional loss is an order of magnitude lower than the stringent 0.4 bar allowable system limit, thereby guaranteeing significant reductions in parasitic pumping power requirements and minimizing the risk of pump cavitation.

Thermally, the numerical simulations validated the efficacy of the conjugate heat transfer mechanism under severe multi-source localized heat flux conditions and an aggressive 50°C ambient environment. The LCP demonstrated excellent thermal spreading capabilities, restricting the maximum fluid temperature rise to just 2°C. Consequently, the maximum plate surface temperature was successfully maintained at 37.2°C, which strictly satisfies the critical 40°C operational threshold required to prevent semiconductor degradation and thermal runaway.

Ultimately, the proposed monolithic deep-drilled cold plate circumvents the structural vulnerabilities and internal thermal resistances characteristic of traditional brazed or swaged tube designs. By satisfying both stringent hydraulic constraints and rigorous thermal limits, the proposed system demonstrates strong potential as a highly reliable, compact, and efficient active cooling solution for next-generation high heat flux electronic applications, including laser diodes, insulated-gate bipolar transistors (IGBTs), and industrial power converters.

REFERENCES

[1] S. V. Garimella *et al.*, "Thermal Challenges in Next-Generation Electronic Systems," *IEEE Transactions on Components, Packaging and Manufacturing Technology*, vol. 2, no. 8, pp. 1326-1335, 2012.
[2] C. Lasance, "The limits of air cooling in electronics," *Proceeding of the 11th International Symposium on Thermal and Polymeric Materials*, 2005.
[3] A. Faghri, "Heat pipes: Review, opportunities and challenges," *Frontiers in Heat and Mass Transfer (FHMT)*, vol. 5, no. 1, 2014.
[4] I. Mudawar, "Assessment of high-heat-flux thermal management schemes," *IEEE Transactions on Components and Packaging Technologies*, vol. 24, no. 1,

International Journal of Engineering Research & Technology (IJERT)
ISSN: 2278-0181
Vol. 15 Issue 04 , April - 2026

pp. 122-141, 2001.

[5] D. B. Tuckerman and R. F. W. Pease, "High-performance heat sinking for VLSI," *IEEE Electron Device Letters*, vol. 2, no. 5, pp. 126-129, 1981.

[6] J. Wei *et al.*, "Heat transfer and pressure drop characteristics of serpentine mini-channel liquid cold plates," *Applied Thermal Engineering*, vol. 124, pp. 1046-1055, 2017.

[7] H. Wang *et al.*, "Reliability of Liquid Cooling Systems in Power Electronics: A Review," *International Journal of Heat and Mass Transfer*, vol. 118, pp. 879-892, 2018.

[8] T. L. Bergman, A. S. Lavine, F. P. Incropera, and D. P. DeWitt, *Fundamentals of Heat and Mass Transfer*, 7th ed. Hoboken, NJ: John Wiley & Sons, 2011.

[9] A. Bejan, *Convection Heat Transfer*, 4th ed. Hoboken, NJ: John Wiley & Sons, 2013.

[10] S. G. Kandlikar, *Liquid Cooling of Electronic Devices by Single-Phase Convection*, New York, NY: John Wiley & Sons, 1999.

[11] *ANSYS Fluent Theory Guide*, Release 2021 R1, ANSYS, Inc., Canonsburg, PA, 2021.